

## Effect of the Spacer Moiety on the Rates of Electron Transfer within Bis-Porphyrin-Stoppered Rotaxanes

Jean-Claude Chambron,<sup>†</sup> Anthony Harriman,<sup>\*‡</sup> Valérie Heitz,<sup>†‡</sup> and Jean-Pierre Sauvage<sup>\*†</sup>

Contribution from the Faculté de Chimie, Université Louis Pasteur, 67000 Strasbourg, France, and Center for Fast Kinetics Research, The University of Texas at Austin, Austin, Texas 78712

Received February 17, 1993

**Abstract:** A set of rotaxanes has been constructed consisting of a 30-membered macrocyclic ring, incorporating a 2,9-diphenyl-1,10-phenanthroline residue, threaded onto a second 2,9-diphenyl-1,10-phenanthroline residue with gold(III) and zinc(II) porphyrins acting as terminal stoppers. The two chelating groups may be coordinated to copper(I) or zinc(II) cations or left free. Upon selective excitation of either porphyrin, rapid electron transfer occurs from the zinc porphyrin to the appended gold porphyrin and the ground state is restored by relatively slow reverse electron transfer. The rates of the various electron-transfer steps show a marked dependence on the molecular architecture and may be understood in terms of a frontier molecular orbital energy diagram involving through-bond electron or hole transfer. The coordinating cation modulates the energy of orbitals on the spacer and, thereby, affects the rate of electron transfer. The central metal complex may also be involved as a "real" intermediate in the electron-transfer pathway. Compared to the corresponding bis-porphyrin, rates of electron transfer at zero activation free energy change and the magnitude of electronic coupling between the porphyrins are significantly lower in the rotaxanes. This may be a consequence of subtle changes in the stereochemistry.

An important aspect in furthering our understanding of the intimate details about electron-transfer processes concerns the role of the intervening medium that lies between a donor and its complementary acceptor.<sup>1</sup> In the bacterial photosynthetic reaction center complex, for example, an accessory bacteriochlorophyll molecule is located between the dimeric bacteriochlorophyll donor and the bacteriopheophytin acceptor.<sup>2</sup> It is believed that mixing between orbitals on this accessory bacteriochlorophyll molecule and those on the donor and acceptor results in enhanced rates of electron transfer from the donor to the acceptor.<sup>3</sup> It has also been suggested that the accessory bacteriochlorophyll acts as a "real", as opposed to a "virtual", intermediate in the electron-transfer process.<sup>4</sup> The two mechanisms may operate simultaneously,<sup>5</sup> but since they are expected to exhibit distinct activation energies, their fractional contribution may depend on temperature.<sup>6</sup> Similar ideas have been raised regarding long-range electron transfer through protein matrices where aromatic residues on tyrosine, tryptophan, or phenylalanine may provide preferred pathways.<sup>7</sup> Studies with covalently-linked donor-acceptor compounds have improved our knowledge of how electronic coupling

between the subunits depends on the length,<sup>8</sup> stereochemistry,<sup>9</sup> and energetics<sup>10</sup> of the spacer moiety. However, it has been difficult to design sets of model compounds which clearly demonstrate the "superexchange" effect for photoinduced electron transfer,<sup>11</sup> although it has been established that spacers having low-energy  $\pi$ -electron systems facilitate rapid electron transfer.<sup>12</sup>

We have reported earlier that photoinduced electron transfer between zinc(II) and gold(III) porphyrinic subunits separated by a covalently-attached 2,9-diphenyl-1,10-phenanthroline spacer moiety proceeds by way of LUMO or HOMO orbitals located on the spacer.<sup>13,14</sup> These orbitals lie at relatively low energy and can mix with accepting and donating orbitals on the porphyrinic subunits. In principle, the energy of these molecular orbitals can be modulated by coordination of the 1,10-phenanthroline residue

(8) (a) Hush, N. S.; Paddon-Row, M. N.; Cotsaris, E.; Oevering, H.; Verhoeven, J. W.; Heppener, M. *Chem. Phys. Lett.* **1985**, *117*, 8. (b) Warman, J. M.; de Haas, M. P.; Paddon-Row, M. N.; Cotsaris, E.; Hush, N. S.; Oevering, H.; Verhoeven, J. W. *Nature* **1986**, *320*, 615. (c) Closs, G. L.; Calcaterra, L. T.; Green, N. S.; Penfield, K. W.; Miller, J. R. *J. Phys. Chem.* **1986**, *90*, 3673. (d) Johnson, M. D.; Miller, J. R.; Green, N. S.; Closs, G. L. *J. Phys. Chem.* **1989**, *93*, 1173.

(9) (a) Wegewijs, B.; Hermant, R. M.; Verhoeven, J. W.; Kunst, A. G. M.; Rettschnick, R. P. H. *Chem. Phys. Lett.* **1987**, *140*, 587. (b) Wegewijs, B.; Hermant, R. M.; Verhoeven, J. W.; de Haas, M. P.; Warman, J. M. *Chem. Phys. Lett.* **1990**, *168*, 185. (c) Delaney, J. K.; Mauzerall, D. C.; Lindsey, J. S. *J. Am. Chem. Soc.* **1990**, *112*, 957. (d) Sakata, Y.; Nakashima, S.; Goto, Y.; Tatsumi, H.; Misumi, S. *J. Am. Chem. Soc.* **1989**, *111*, 8978. (e) Closs, G. L.; Calcaterra, L. T.; Green, N. S.; Penfield, K. W.; Miller, J. R. *J. Phys. Chem.* **1986**, *90*, 3673.

(10) (a) Beratan, D. N.; Onuchic, J. N.; Hopfield, J. J. *J. Chem. Phys.* **1985**, *83*, 5325. (b) Beratan, D. N. *J. Am. Chem. Soc.* **1986**, *108*, 4321. (c) Ratner, M. A. *J. Phys. Chem.* **1990**, *94*, 4877. (d) Siddarth, P.; Marcus, R. A. *J. Phys. Chem.* **1990**, *94*, 2985.

(11) Wasielewski, M. R.; Niemczyk, M. P.; Johnson, D. G.; Svec, W. A.; Minsek, D. W. *Tetrahedron* **1989**, *45*, 4785.

(12) (a) Heitele, H.; Michel-Beyerle, M. E. *J. Am. Chem. Soc.* **1985**, *107*, 8286. (b) Heiler, D.; McLendon, G.; Rogalskyj, P. *J. Am. Chem. Soc.* **1987**, *109*, 604. (c) Finckh, P.; Heitele, M.; Volk, M.; Michel-Beyerle, M. E. *J. Phys. Chem.* **1988**, *92*, 6584. (d) Osuka, A.; Maruyama, K.; Mataga, M.; Asahi, T.; Yamazaki, I.; Tamai, N. *J. Am. Chem. Soc.* **1990**, *112*, 4958.

(13) Brun, A. M.; Harriman, A.; Heitz, V.; Sauvage, J.-P. *J. Am. Chem. Soc.* **1991**, *113*, 8657.

(14) Harriman, A.; Heitz, V.; Sauvage, J.-P. *J. Phys. Chem.* **1993**, *97*, 5940.

<sup>†</sup> Université Louis Pasteur.

<sup>‡</sup> The University of Texas at Austin.

(1) Miller, J. R. *Now. J. Chim.* **1987**, *11*, 83.

(2) (a) Deisenhofer, J.; Epp, O.; Miki, K.; Huber, R.; Michel, H. *J. Mol. Biol.* **1984**, *180*, 385. (b) Deisenhofer, J.; Epp, O.; Miki, K.; Huber, R.; Michel, H. *Nature* **1985**, *318*, 618.

(3) (a) Bixon, M.; Jortner, J.; Michel-Beyerle, M. E.; Ogrodnik, A.; Lersch, W. *Chem. Phys. Lett.* **1987**, *140*, 626. (b) Creighton, S.; Hwang, J. K.; Warshel, A.; Parson, W. W.; Norris, J. R. *Biochemistry* **1988**, *27*, 774. (c) Plato, M.; Mobius, K.; Michel-Beyerle, M. E.; Bixon, M.; Jortner, J. *J. Am. Chem. Soc.* **1988**, *110*, 7279. (d) Bixon, M.; Jortner, J.; Michel-Beyerle, M. E.; Ogrodnik, A. *Biochim. Biophys. Acta* **1989**, *977*, 273.

(4) (a) Haberkorn, R.; Michel-Beyerle, M. E.; Marcus, R. A. *Proc. Natl. Acad. Sci. U.S.A.* **1979**, *76*, 4185. (b) Marcus, R. A. *Chem. Phys. Lett.* **1987**, *133*, 471.

(5) (a) Bixon, M.; Jortner, J.; Michel-Beyerle, M. E. *Biochim. Biophys. Acta* **1991**, *1056*, 301. (b) Joseph, J.; Bruno, W.; Bialek, W. *J. Phys. Chem.* **1991**, *95*, 6242.

(6) Jortner, J.; Bixon, M. In *Dynamics and Mechanisms of Photoinduced Electron Transfer and Related Phenomena*; Mataga, N.; Okada, T.; Masuhara, H., Eds.; Elsevier: Amsterdam, 1992; p 513.

(7) (a) Isied, S. S. *Prog. Inorg. Chem.* **1984**, *32*, 443. (b) Onuchic, J. N.; Beratan, D. N. *J. Chem. Phys.* **1990**, *92*, 722.

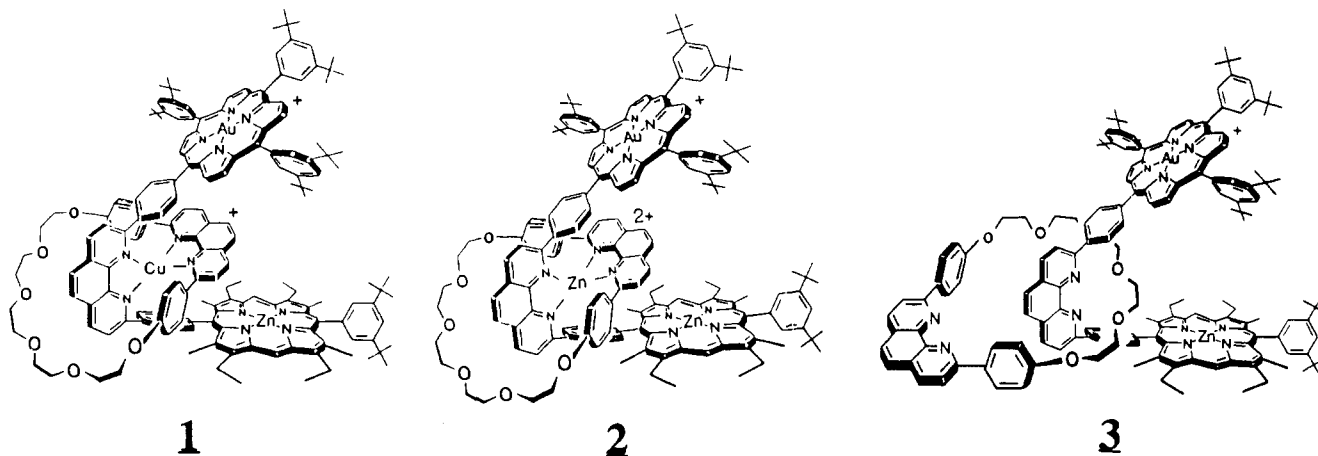


Figure 1. Structures of the rotaxanes.

to appropriate cations<sup>15</sup> in a manner that does not affect the geometry of the bis-porphyrin or the reaction exergonicity for net electron transfer. As such, this approach may enable determination of the effectiveness of the superexchange mechanism at promoting photoinduced electron transfer.<sup>16</sup> We describe here the results of such experiments. It is seen that, as with the bacterial reaction center complex, the spacer moiety can participate in the electron-transfer process as a virtual or real intermediate.

### Experimental Section

Butyronitrile (Aldrich) was fractionally distilled from  $\text{KMnO}_4$  and  $\text{CaCO}_3$ . All other solvents were redistilled from appropriate drying agents. Structures of the rotaxanes 1–3 are given in Figure 1. Synthesis of 1 has been described previously,<sup>17a</sup> and synthetic details for compounds 2 and 3 will be described elsewhere.<sup>17b</sup>

All experiments were made with freshly prepared, dilute solutions of the compound in deoxygenated solvent. Absorption spectra were recorded with a Hitachi U3210 spectrophotometer. Luminescence spectra were recorded with a Perkin Elmer LS5 spectrofluorimeter and were corrected for wavelength responses of the detector. Fluorescence quantum yields were measured relative to zinc tetraphenylporphyrin (ZnTPP) ( $\Phi_f = 0.033$ ).<sup>18</sup> Singlet excited state lifetimes were measured by time-correlated, single-photon counting using a mode-locked Nd-YAG laser (Antares 76S) synchronously pumping a cavity-dumped Rhodamine 6G dye laser (Spectra Physics 375B/244). A high-radiance monochromator and pinhole attachment were used to isolate fluorescence from scattered laser light. A Hamamatsu microchannel plate was used to detect emitted photons, for which the instrumental response function had an fwhm of  $60 \pm 10$  ps. Data analyses were made at six different emission wavelengths using global analysis methodology after computer deconvolution of the instrument response function.<sup>19</sup> Variable-temperature studies were made with an optical dewar cooled or heated with a stream of  $\text{N}_2$ . The temperature was recorded with a thermocouple in contact with the solution and was accurate to  $\pm 0.2$  °C.

Flash photolysis studies were made with a frequency-doubled, mode-locked Quantel YG402 Nd-YAG laser (pulse width 30 ps). Laser intensities were attenuated with crossed polarizers, and 300 laser shots were averaged for each measurement. Solutions were adjusted to possess absorbances of ca. 0.4 at the excitation wavelength. Residual 1064-nm output from the laser was focused into 1/1  $\text{D}_3\text{PO}_4/\text{D}_2\text{O}$  to produce a white light continuum for use as the analyzing beam. Variable delay times in the range 0–6 ns were selected in a random sequence, and transient differential absorption spectra were recorded with an Instruments SA UFS200 spectrograph interfaced to a Tracor Northern 6200 MCA and a microcomputer. Kinetic analyses were made by overlaying about 40

individual spectra and fitting data at selected wavelengths using computer nonlinear least-squares iterative procedures after deconvolution of the instrument response function.

Improved time resolution was achieved using a frequency-doubled, mode-locked Antares 76S Nd-YAG laser to pump a Coherent 700 dual jet (Rhodamine 6G) dye laser operated at 76 MHz. A Quantel model RGA67-10 regenerative amplifier, a Quantel model PTA-60 dye laser, and a Continuum SPA1 autocorrelator were used to obtain 3-mJ pulses at 586 nm having an fwhm of ca. 500 fs. The spectrometer was run at a frequency of 10 Hz, and data were acquired through a Princeton dual diode array spectrograph interfaced to a microcomputer. The detection setup and optical delay line were similar to those used for the 30-ps pulse width experiments; in both cases, the exciting and analyzing beams were almost collinear. Again, kinetic analyses were made by overlaying spectra collected at about 50 different delay times.

Redox potentials for one-electron oxidation or reduction of the porphyrinic subunits were derived by cyclic voltammetry in deoxygenated butyronitrile containing tetra-*n*-butylammonium perchlorate (0.2 M). A glassy carbon working electrode was used in conjunction with a Pt counter electrode and an SCE reference electrode. The peaks were assigned to particular processes on the basis of measurements made with appropriate model compounds.<sup>13,14</sup> The redox potential for one-electron reduction of the gold(III) porphyrinic subunit was found to be  $-0.52 \pm 0.05$  V vs SCE. The redox potential for one-electron oxidation of the zinc(II) porphyrinic subunit was found to be  $0.68 \pm 0.04$  V vs SCE. The redox potential for one-electron oxidation of the copper(I) complex in 1 was found to be  $0.55 \pm 0.04$  V vs SCE. Redox potentials for one-electron reduction and oxidation, respectively, of 2,9-diphenyl-1,10-phenanthroline were found to be  $-2.00 \pm 0.04$  and  $1.95 \pm 0.05$  V vs SCE. The parallel values for copper(I) bis(2,9-diphenyl-1,10-phenanthroline) were  $-1.65 \pm 0.05$  and  $1.80 \pm 0.05$  V vs SCE, respectively. The corresponding values for zinc-(II) bis(2,9-diphenyl-1,10-phenanthroline) were  $-0.95 \pm 0.03$  and  $1.93 \pm 0.05$  V vs SCE, respectively. Excited-state energy levels were determined from luminescence spectra recorded in ethanol at 77 K. The excited singlet state energy of the zinc(II) porphyrin subunit was found to be 2.18 eV, and the excited triplet state energy of the gold(III) porphyrin subunit was found to be 1.82 eV.

### Results

**Excitation of the Rotaxanes via the Zinc(II) Porphyrin Subunit in Butyronitrile.** Upon excitation at 586 nm, where only the zinc porphyrin subunit absorbs, extremely weak fluorescence could be observed. The fluorescence spectrum corresponded to emission from a zinc porphyrin,<sup>18</sup> and the excitation spectrum recorded over the visible region resembled that found for the model zinc porphyrin. Fluorescence quantum yields ( $\Phi_f$ ), determined by comparison with an optically-matched solution of zinc tetraphenylporphyrin, were  $<10^{-3}$  for all three rotaxanes (Table I). The fluorescence decay profiles recorded for 1 by time-correlated, single-photon counting techniques could not be properly resolved from the instrument response function. The excited singlet state lifetime ( $\tau_s$ ) for the zinc porphyrin subunit in this compound, therefore, is  $<10$  ps. For 2 and 3, fluorescence from the zinc

(15) Dietrich-Buchecker, C.; Sauvage, J.-P.; Kern, J.-M. *J. Am. Chem. Soc.* **1989**, *111*, 7791.

(16) Wasielewski, M. R. *Chem. Rev.* **1992**, *92*, 495.

(17) (a) Chambron, J.-C.; Heitz, V.; Sauvage, J.-P. *J. Chem. Soc., Chem. Commun.* **1992**, 1131. (b) Chambron, J.-C.; Heitz, V.; Sauvage, J.-P. *J. Am. Chem. Soc.*, to be submitted.

(18) Ergorova, G. D.; Knyukshto, V. N.; Solovov, K. N.; Tsvirko, M. P. *Opt. Spectrosc. (Engl. Transl.)* **1980**, *48*, 602.

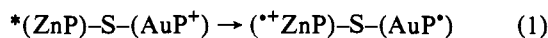
(19) Knutson, J.; Beechem, J.; Brand, L. *Chem. Phys. Lett.* **1983**, *102*, 501.

**Table I.** Photophysical Properties Measured for the Rotaxanes and the Corresponding Bis-Porphyrin (**4**) in Butyronitrile at 25 °C

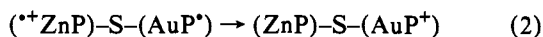
compound	$\Phi_f$	$\tau_s$ (ps)	$\tau_t$ (ps)	$\tau_{cts}$ (ps)
<b>1</b>	<0.001	1.7	17	22
<b>2</b>	<0.001	28	56	360
<b>3</b>	<0.001	36	71	540
<b>4</b>	0.001	55	120	580

porphyrin subunit could be time-resolved and the corresponding excited singlet state lifetimes were found to be  $28 \pm 4$  and  $36 \pm 3$  ps, respectively (Table I). The corresponding value for the model zinc porphyrin was  $1.9 \pm 0.1$  ns.

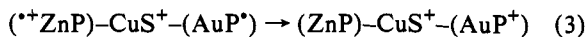
Immediately after excitation of **2** or **3** in butyronitrile with a 0.5-ps laser pulse at 586 nm, the characteristic differential absorption spectral features of the excited singlet state of the zinc porphyrin were observed.<sup>13,14,20</sup> This state decayed rapidly, with lifetimes of  $22 \pm 3$  and  $34 \pm 4$  ps, respectively, for **2** and **3**, to form the charge-transfer state (CTS) consisting of the zinc porphyrin  $\pi$ -radical cation and the gold(III) porphyrin neutral radical.<sup>13,14</sup> This CTS is formed upon electron transfer from the excited singlet state of the zinc(II) porphyrin to the appended gold(III) porphyrin; the reaction exothermicity ( $\Delta G^\circ$ ) for this reaction is  $-0.98$  eV.<sup>21</sup>



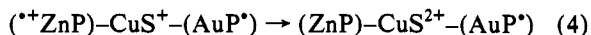
The CTS decayed on a relatively slow time scale to regenerate the ground state system ( $\Delta G^\circ = -1.20$  eV). The lifetimes for the CTS ( $\tau_{cts}$ ), measured at various wavelengths across the spectrum, are compiled in Table I.



Under identical conditions, the zinc porphyrin excited singlet state could not be properly resolved for **1**, and within a few ps of excitation, the observed differential absorption spectrum was characteristic of the CTS.<sup>22,23</sup> Stimulated emission from the zinc porphyrin subunit, detected at 620 nm, was found to decay with a lifetime of  $1.7 \pm 0.4$  ps. In addition, monitoring at 660 nm, where the charge-transfer state has a pronounced absorption relative to the excited singlet state, it was observed that formation of the CTS occurred by first-order kinetics with a lifetime of  $1.5 \pm 0.5$  ps. In this case, the CTS decayed by first-order kinetics ( $\tau_{cts} = 22 \pm 4$  ps) to leave a residual species having the characteristic differential absorption spectrum of the gold(III) porphyrin neutral radical. Deactivation of the CTS may be considered<sup>22</sup> to involve both direct reverse electron transfer between porphyrinic species ( $\Delta G^\circ = -1.20$  eV)



and/or electron transfer from the central copper(I) complex to the zinc porphyrin  $\pi$ -radical cation ( $\Delta G^\circ = -0.13$  eV).<sup>24</sup>



On the basis of differential extinction coefficients measured previously, the latter process appears to be quantitative,<sup>23</sup> despite its minimal thermodynamic driving force. The residual gold(III) porphyrin neutral radical decayed on a much longer time scale due to electron donation to the copper(II) complex ( $\Delta G^\circ$

(20) Rodriguez, J.; Kirmaier, C.; Holten, D. *J. Am. Chem. Soc.* **1989**, *111*, 6500.

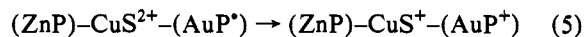
(21) Calculated according to  $\Delta G^\circ = -F\{E_A^\circ - (E_D^\circ - E_s)\}$ , where  $E_A^\circ$  and  $E_D^\circ$  refer respectively to the one-electron redox potentials for reduction of the gold(III) porphyrin and for oxidation of the zinc(II) porphyrin and  $E_s$  is the excitation energy of the zinc(II) porphyrin first excited singlet state.

(22) Brun, A. M.; Atherton, S. J.; Harriman, A.; Heitz, V.; Sauvage, J.-P. *J. Am. Chem. Soc.* **1992**, *114*, 4632.

(23) Chambon, J.-C.; Harriman, A.; Heitz, V.; Sauvage, J.-P. *J. Am. Chem. Soc.*, in press.

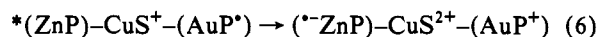
(24) Calculated according to  $\Delta G^\circ = -F\{E_D^\circ - E_{Cu}^\circ\}$ , where  $E_D^\circ$  and  $E_{Cu}^\circ$  refer respectively to the one-electron redox potentials for oxidation of the zinc(II) porphyrin and the central copper(I) complex.

$= -1.07$  eV).

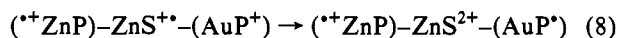
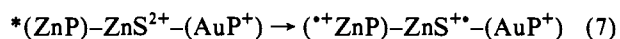


The rate constant for reaction 5 ( $k_5$ ) was found to be  $(4.0 \pm 0.8) \times 10^8$  s<sup>-1</sup>. It should be noted that the central zinc(II) complex in the rotaxane **2** is not oxidized by the zinc porphyrin  $\pi$ -radical cation because of the high reaction endothermicity ( $\Delta G^\circ = >1$  eV).

On the basis of redox potentials measured for the various compounds, it is necessary to consider two other electron-transfer processes. First, the zinc porphyrin excited singlet state might be expected to oxidize the central copper(I) complex in the rotaxane **1** since there is a modest thermodynamic driving force for this process ( $\Delta G^\circ = -0.08$  eV).<sup>25</sup>

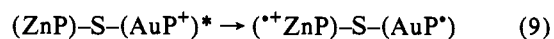


The characteristic transient differential absorption spectrum of the zinc porphyrin  $\pi$ -radical anion<sup>26</sup> is not observed, however, and it is clear that this reaction does not compete with reaction 1. Second, the zinc porphyrin excited singlet state might be expected to reduce the central zinc(II) complex in the rotaxane **2** ( $\Delta G^\circ = -0.55$  eV),<sup>27</sup> followed by reduction of the appended gold(III) porphyrin ( $\Delta G^\circ = -0.43$  eV).



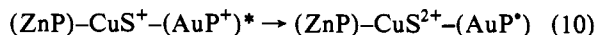
This two-step mechanism may operate for rotaxane **2**, but we could not detect the intermediate formation of the (ligand-localized) zinc(I) complex. Spectroelectrochemical studies have shown<sup>15</sup> that this latter species exhibits a weak absorption band centered around 530 nm with a molar extinction coefficient of  $\approx 1000$  M<sup>-1</sup> cm<sup>-1</sup>. This band would be hidden by the more intense spectral changes associated with the porphyrinic subunits.

**Excitation of the Rotaxanes via the Gold(III) Porphyrin Subunit in Butyronitrile.** Excitation of compounds **1–3** with a 30-ps laser pulse at 532 nm, where the gold(III) porphyrin subunit absorbs about 80% of the total incident photons, resulted in formation of the gold(III) porphyrin triplet excited state.<sup>13,14</sup> This species decayed rapidly to form the CTS ( $\Delta G^\circ = -0.62$  eV), as detected by its characteristic transient differential absorption spectrum.



After deconvolution of the laser pulse, the lifetime of the gold(III) porphyrin excited triplet state ( $\tau_t$ ) was determined and the derived values are collected in Table I; the value measured for the corresponding model porphyrin was  $1.5 \pm 0.2$  ns. The CTS decayed as described for excitation into the zinc porphyrinic subunit.

Again, it is necessary to consider an alternative reaction. Thus, the triplet excited state of the gold(III) porphyrin might be expected to oxidize the central copper(I) complex in the rotaxane **1** since there is a significant thermodynamic driving force for this process ( $\Delta G^\circ = -0.75$  eV).



The observed transient differential absorption spectral changes, however, are inconsistent with reaction 10 being the sole means

(25) Calculated according to  $\Delta G^\circ = -F\{(E_A^\circ + E_s) - E_D^\circ\}$ , where  $E_A^\circ$  and  $E_D^\circ$  refer respectively to the one-electron redox potentials for reduction of the zinc(II) porphyrin ( $E_A^\circ = -1.55$  V vs SCE) and for oxidation of the central copper(I) complex and  $E_s$  is the excitation energy of the zinc(II) porphyrin first excited singlet state.

(26) Closs, G. L.; Closs, L. E. *J. Am. Chem. Soc.* **1963**, *85*, 818.

(27) Calculated according to  $\Delta G^\circ = -F\{E_A^\circ - (E_D^\circ - E_s)\}$ , where  $E_A^\circ$  and  $E_D^\circ$  refer respectively to the one-electron redox potentials for reduction of the central zinc(II) complex and oxidation of the zinc(II) porphyrin and  $E_s$  is the excitation energy of the zinc(II) porphyrin first excited singlet state.

by which the gold porphyrin excited triplet state is quenched. Even so, we cannot rule out the possibility that reaction 10 contributes toward the overall quenching reaction and, on the basis of rate constants measured for comparable systems,<sup>22</sup> we estimate that reaction 10 accounts for about 10% of triplet deactivation. We attribute the relative slowness of this reaction to a high reorganization energy<sup>28</sup> associated with formation of a coordinatively unsaturated copper(II) complex.

**Effect of Temperature on the Rates of Electron Transfer for 3.** Direct involvement of the central metal complex in the overall redox chemistry may complicate data analysis for the copper(I) rotaxane **1** and the zinc(II) rotaxane **2**. Consequently, the metal-free rotaxane **3** was selected for detailed investigation into the effects of temperature and solvent polarity on the rates of photoinduced and reverse electron-transfer processes. The purpose of these studies is to determine the magnitude of the electronic coupling matrix element ( $V$ ) and the solvent reorganization energy ( $\lambda_S$ ) for comparison with values measured for the corresponding bis-porphyrin under similar conditions.<sup>14</sup>

For a nonadiabatic electron-transfer reaction, the rate constant ( $k$ ) can be expressed in the following form:<sup>29</sup>

$$k = (4\pi^2/h)V^2(\text{FCWD}) \quad (11a)$$

$$\text{FCWD} = [4\pi\lambda_S k_B T]^{-1/2} \sum_{w=0}^{\infty} (e^{-S} S^w / w!) \times \exp\{-(\lambda_S + \Delta G^\circ + whc\nu)^2 / 4\lambda_S k_B T\} \quad (11b)$$

$$S = \lambda_V / hc\nu \quad (11c)$$

Here,  $\lambda_V$  refers to the nuclear reorganization energy,  $k_B$  is the Boltzmann constant,  $c$  is the speed of light, and  $\nu$  is a single average skeletal vibration of 1500  $\text{cm}^{-1}$ . This expression can be rewritten in the form of an Arrhenius-type equation:<sup>30</sup>

$$\ln [kT^{1/2}] = \ln A - (\Delta H^* / RT) \quad (12a)$$

$$A = \{(4\pi^2 V^2 / h)[4\pi\lambda_S k_B]^{-1/2}\} \exp^{-S} \quad (12b)$$

Here,  $\Delta H^*$  refers to the activation enthalpy, as defined by eq 11. In applying eq 12, we assume that the conformation of the rotaxane and the reaction exothermicity remain independent of temperature. This is particularly important for the cation-free rotaxane **3** where the accessory 1,10-phenanthroline residue might rotate around the porphyrin stoppers.<sup>31</sup> Consequently, we have restricted the maximum temperature to 70 °C. In support of the latter assumption, we expect there to be only a small entropy change associated with the various electron-transfer processes since a charge shift between porphyrinic species destroys a solvation environment around one porphyrin but creates a similar one around the other porphyrin.<sup>32</sup> It is also important to note that for butyronitrile the solvent reorganization energy ( $\lambda_S$ ) is insensitive to temperature and varies by less than 5% over the temperature range under investigation.<sup>14</sup>

Rate constants for each of the various electron-transfer steps following from selective excitation into one of the porphyrinic subunits were measured in butyronitrile over the temperature range -90–70 °C. Figure 2 shows Arrhenius-type plots for each of the electron-transfer processes; namely, photoinduced electron

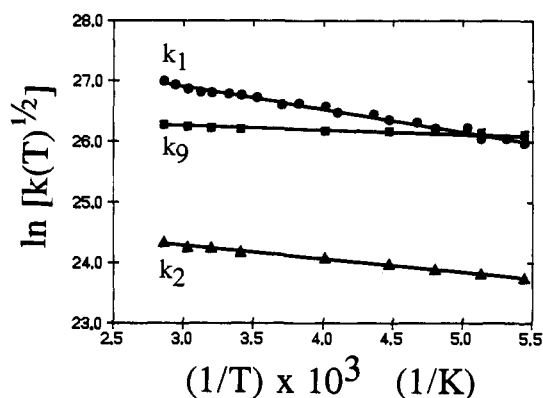


**Figure 2.** Arrhenius-type plots for the effect of temperature on the rates of electron transfer occurring for **3** in butyronitrile for photoinduced electron transfer from the excited singlet state of the zinc porphyrin (●) and the excited triplet state of the gold(III) porphyrin (■) and for reverse electron transfer (▲). The solid line drawn through each set of data points is the best fit to eq 12.

**Table II.** Activation Enthalpies, Solvent Reorganization Energies, and Electronic Matrix Coupling Elements Derived from the Temperature-Dependence Studies in Butyronitrile and the Slopes and Maximum Rate Constants Derived from the Solvent-Dependence Studies for the Solvents Listed in Table III<sup>a</sup>

reaction <sup>b</sup>	$\Delta H^*$ (eV)	$\lambda_S$ (eV)	$V$ ( $\text{cm}^{-1}$ )	slope	$k_0/10^9$ ( $\text{s}^{-1}$ )
Rotaxane <b>3</b>					
1	0.032	0.69	30	-0.52	50
2	0.019	0.93	6	-0.26	3.6
9	0.003	0.73	12	-0.44	17
Bis-Porphyrin <b>4</b>					
1	0.090	1.47	85	-0.81	160
2	0.003	1.31	5	-0.97	1.7
9	0.130	1.33	110	-0.83	42

<sup>a</sup> Data refer to rotaxane **3** and the corresponding bis-porphyrin **4**.  
<sup>b</sup> Refers to the reaction number in the text.

transfer from the excited singlet state of the zinc porphyrin ( $k_1$ ), photoinduced electron abstraction by the excited triplet state of the gold(III) porphyrin ( $k_9$ ), and reverse electron transfer ( $k_2$ ). Linear plots to eq 12 were observed in each case, and values for the activation enthalpies, as derived from the slopes, are collected in Table II. The solid line drawn through each set of data points represents the best fit to eq 11, and the derived values for the solvent reorganization energy ( $\lambda_S$ ) are collected in Table II. The average value for  $\lambda_S$  for the photoinduced electron-transfer processes is  $0.71 \pm 0.05$  eV, and this is very much lower than that observed for the corresponding bis-porphyrin ( $\lambda_S = 1.36$  eV).<sup>14</sup> A higher value ( $\lambda_S = 0.93 \pm 0.05$  eV) was observed for the charge recombination process, but this reaction is expected to fall within the onset of the inverted region where anomalously low activation energies are known to occur.<sup>33</sup> Using  $\lambda_S = 0.71$  eV, the magnitude of the electronic coupling matrix element ( $V$ ) was calculated for each process from the intercepts of Figure 2 and the derived values are compiled in Table II. For the purpose of this latter calculation, the nuclear reorganization energy ( $\lambda_V$ ) was assumed to be 0.20 eV.<sup>14</sup> Again, for the photoinduced processes, the values are significantly lower than those observed for the corresponding bis-porphyrin whereas the values are very similar for reverse electron transfer.

**Effect of Solvent Polarity on the Rates of Electron Transfer for 3.** Rate constants for electron transfer occurring via the first excited singlet state of the zinc porphyrin ( $k_1$ ), via the excited triplet state of the gold porphyrin ( $k_9$ ), and for reverse electron transfer ( $k_2$ ) were measured in a range of solvents at 25 °C. The

(28) (a) Blaskie, M. W.; McMillan, D. R. *Inorg. Chem.* **1980**, *19*, 3519. (b) Palmer, C. E. A.; McMillan, D. R.; Kirmaier, C.; Holten, D. *Inorg. Chem.* **1987**, *26*, 3167.

(29) (a) Marcus, R. A. *Ann. Rev. Phys. Chem.* **1964**, *15*, 155. (b) Levich, V. G.; Dogonadze, R. R. *Collect. Czech. Chem. Commun.* **1961**, *26*, 193. (c) Kestner, N. R.; Lofan, J.; Jortner, J. *J. Phys. Chem.* **1974**, *78*, 2148.

(30) Lin, J. Y.; Bolton, J. R. *J. Phys. Chem.* **1992**, *96*, 1718.

(31) That the accessory 1,10-phenanthroline residue lies away from the porphyrin subunits was clearly demonstrated by <sup>1</sup>H NMR studies.<sup>17b</sup>

(32) Miller, J. R.; Beitz, J. V. *J. Chem. Phys.* **1981**, *74*, 6746.

(33) (a) Liang, N.; Miller, J. R.; Closs, G. L. *J. Am. Chem. Soc.* **1989**, *111*, 8740. (b) Liang, N.; Miller, J. R.; Closs, G. L. *J. Am. Chem. Soc.* **1990**, *112*, 5353.

**Table III.** Solvent Reorganization Energies and Rate Constants for Electron Transfer for Rotaxane 3 in a Series of Solvents at 25 °C

solvent	$\lambda_S$ (eV)	$\log k_1$	$\log k_2$	$\log k_9$
CH <sub>3</sub> OH	0.80	10.74	9.50	10.10
C <sub>2</sub> H <sub>5</sub> OH	0.75	10.85	9.36	10.11
CH <sub>3</sub> CN	0.79	10.76	9.36	10.08
DMF <sup>a</sup>	0.70	10.49	9.26	10.16
PC <sup>b</sup>	0.72	10.59	9.30	10.15
acetone	0.74	10.47	9.31	10.13
BCN <sup>c</sup>	0.71	10.49	9.27	10.15
CH <sub>2</sub> Cl <sub>2</sub>	0.57	10.21	8.90	10.22
DMSO <sup>d</sup>	0.66	10.44	9.23	10.22
CHCl <sub>3</sub>	0.40	9.41		10.06
CH <sub>2</sub> ClCH <sub>2</sub> Cl	0.56	10.27	8.97	10.22

<sup>a</sup> *N,N*-Dimethylformamide. <sup>b</sup> Propylene carbonate. <sup>c</sup> Butyronitrile. <sup>d</sup> Dimethyl sulfoxide.

derived values are collected in Table III, together with the solvent reorganization energy ( $\lambda_S$ ) for that solvent. The latter value was calculated according to the dielectric continuum model<sup>34</sup> on the basis of  $\lambda_S = 0.71 \pm 0.05$  eV in butyronitrile:

$$\lambda_S = 1.50[(1/\epsilon_{op}) - (1/\epsilon_s)] = 1.50f \quad (13)$$

Here,  $\epsilon_{op}$  and  $\epsilon_s$  refer, respectively, to the optical and static dielectric constants of the solvent at 25 °C.

Equation 11 can be rewritten in the following form which highlights the solvent dependence of the rate of electron transfer:

$$\ln [k(\lambda_S)^{1/2}] = \ln B - (\Delta G^*/k_B T) \quad (14a)$$

$$B = \{ (4\pi^2 V^2/h) [4\pi k_B T]^{-1/2} \} \exp^{-S} \quad (14b)$$

Although individual redox potentials for porphyrinic species are dependent on the nature of the solvent,<sup>35</sup> the differences between oxidation and reduction processes remain reasonably insensitive to changes in solvent. Thus,  $\Delta G^\circ$  is essentially independent of solvent and, consequently, any significant solvent effect on  $\Delta G^*$  can be attributed to modulation of  $\lambda_S$  according to eq 13.

The derived results are plotted in Figure 3 in the form of eq 14. Although there is considerable scatter among the data points, each plot was linear with a slope in the region of  $-1.0$ , as expected from eq 14. The slopes, as calculated by nonlinear least-squares analysis of the data,<sup>36</sup> are provided in Table II. The intercepts<sup>36</sup> also provide valuable information in that they refer to the rate constant for electron transfer at zero activation free energy change ( $k_0$ ). Essentially, this is the maximum value for that particular electron-transfer process and the derived values are provided in Table II. As above, for the photoinduced processes, these values are very much lower than those observed for the corresponding bis-porphyrin whereas the values are comparable for reverse electron transfer.<sup>14</sup>

## Discussion

The purpose of this work is to compare the effects of molecular architecture on the rates of electron transfer between the porphyrin subunits. Two distinct comparisons can be made; namely, comparison of the rates of electron transfer within the series of rotaxanes and comparison of the electron-transfer rates for the cation-free rotaxane 3 and the corresponding bis-porphyrin 4. In comparing results obtained for the rotaxanes 1 and 2, we assume

(34) (a) Hush, N. S. *Trans. Faraday Soc.* **1961**, *57*, 557. (b) Marcus, R. A. *J. Chem. Phys.* **1965**, *43*, 679.

(35) (a) Schmidt, J. A.; Siemiarczuk, A.; Weedon, A. C.; Bolton, J. R. *J. Am. Chem. Soc.* **1985**, *107*, 6112. (b) Kadish, K. M.; Cornillon, J.-L.; Yao, C.-L.; Malinski, T.; Gritzner, G. *J. Electroanal. Chem. Interfacial Electrochem.* **1987**, *235*, 189.

(36) In order to not overweight the single (isolated) point at the highest activation free energy change ( $\Delta G^*/k_B T$ ) in Figure 3a,b, the intercepts and slopes for these plots were calculated by nonlinear least-squares analysis of plots with these particular points omitted. Including these data points does not affect the intercepts but causes small changes in the slopes.

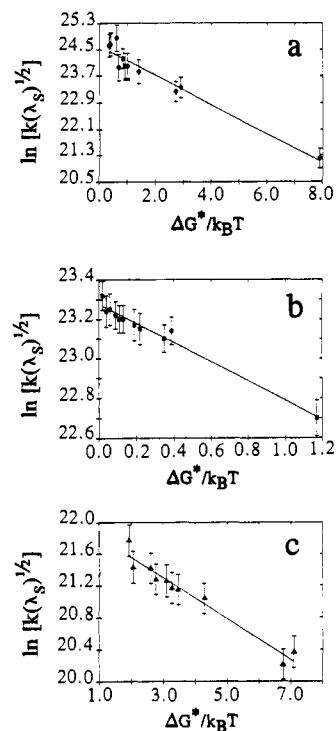


**Figure 3.** Effect of solvent on the rates of electron transfer for 3 at 25 °C for photoinduced electron transfer from the excited singlet state of the zinc porphyrin (a) and the excited triplet state of the gold(III) porphyrin (b) and for reverse electron transfer (c). The solid line drawn through each set of data points is the best fit from least-squares analysis.

a common geometry but we realize that the conformation for 3, which has the accessory 1,10-phenanthroline residue away from the porphyrin rings, may differ somewhat from that of the other rotaxanes. Furthermore, in the detailed analysis of Figure 2, we assume that the average conformation of 3 does not change over the temperature range studied. This rotaxane does not possess a rigid geometry, and we are working in the high-temperature limit where the spacer group may rotate. To what extent the geometry does remain fixed cannot be specified, and it is possible that conformational changes do contribute toward the apparent activation enthalpy. This would also be true for the bis-porphyrin 4. Similarly, the observed solvent effect on the various rates of electron transfer is small (Table III) and, partly because of solubility restrictions, the variation in activation free energy change that can be achieved by changing solvents is modest (Figure 3). It is important, therefore, that interpretation of the experimental data is not overstated and the following analysis is made within these constraints.

For a through-bond electron-transfer process occurring by way of orbitals on the spacer moiety, the electronic matrix coupling element ( $V$ ) can be related to the inverse of the energy gap between donating or accepting orbitals on the porphyrin subunit and the spacer LUMO or HOMO ( $\delta E_{AB}$ ).<sup>37</sup>

$$V = \{ (\beta_{AB}\beta_{BC}) / (\delta E_{AB}) \} \quad (15)$$

Here,  $\beta_{AB}$  and  $\beta_{BC}$  refer, respectively, to electronic coupling factors between orbitals on the initial state and on the spacer moiety and between orbitals on the spacer moiety and on the final state. These latter terms are unknown, but the relevant energy gaps ( $\delta E_{AB}$ ) can be determined from electrochemical measurements. Thus, Figure 4 shows simple frontier molecular orbital diagrams for each of the three electron-transfer processes and indicates the energy gap for electron transfer through the LUMO of the spacer group ( $B_- = \delta E_{AB}$ ) and hole transfer through the HOMO of the spacer moiety ( $B_+ = \delta E_{AB}$ ). The derived values for  $B_-$  and  $B_+$

(37) Larsson, S. *J. Am. Chem. Soc.* **1981**, *103*, 4034.

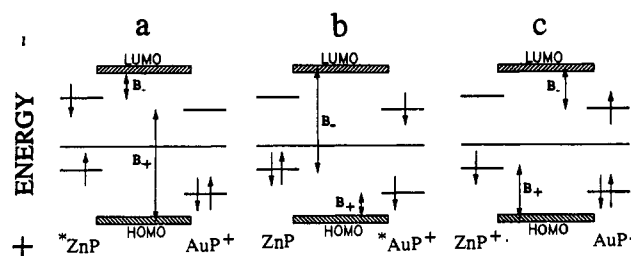


**Figure 4.** MO diagrams illustrating the energy gaps for through-bond electron and hole transfer for the rotaxanes. The systems refer to electron transfer occurring via (a) the excited singlet state of the zinc porphyrin, (b) the triplet excited state of the gold(III) porphyrin, and (c) reverse electron transfer. Values for the energy gaps are collected in Table IV.

**Table IV.** Energy Gaps, Electronic Coupling Terms, and Maximum Rate Constants for **1**

compound	reaction <sup>a</sup>	$B_-$ (eV)	$B_+$ (eV)	$\beta_{AB}\beta_{BC}$ (eV <sup>2</sup> )	$k_0/10^9$ (s <sup>-1</sup> )
1	1	0.15	2.42		
	9	2.33	0.60		
	2	1.13	1.22		
2	1	0.55	2.45		
	9	1.63	0.63		
	2	0.43	1.25		
3	1	0.50	2.47	0.0019	50
	9	2.68	0.65	0.0010	17
	2	1.48	1.27	0.0009	3.6
4	1	0.73	2.52	0.0080	160
	9	2.82	0.65	0.0085	555
	2	1.48	1.16	0.0007	1.7

<sup>a</sup> Refers to the reaction number in the text.

are collected in Table IV. On the assumption that reaction will proceed by way of the process having the smallest energy gap, reaction via the excited singlet state of the zinc porphyrin is expected to involve electron transfer through the LUMO of the spacer. In contrast, reaction via the excited triplet state of the gold porphyrin subunit is expected to involve hole transfer through the HOMO of the spacer moiety. Reverse electron transfer shows no preferred pathway except for the zinc rotaxane **2** where electron transfer through the LUMO of the spacer is the expected route. Identical conclusions were reached for the bis-porphyrin **4**,<sup>14</sup> and it appears that the accessory 1,10-phenanthroline residue does not affect the preferred reaction pathways.

For each of the electron-transfer reactions, there is a rough correlation between the observed rate constant and the inverse of the smallest energy gap ( $B_-$  or  $B_+$ ) as shown in Figure 5a. The derived gradients for these slopes, however, appear to differ significantly, especially for reverse electron transfer. This might be construed to indicate that the  $\beta_{AB}\beta_{BC}$  terms must be quite distinct for each reaction, but too few data points exist for this argument to be developed properly. Furthermore, whereas reverse electron transfer for the zinc rotaxane **2** might be expected to take place via electron transfer through the LUMO of the spacer, that for the other rotaxanes might involve hole transfer via the HOMO of the spacer or through-space electron transfer. There is no reason to suppose that the  $\beta_{AB}\beta_{BC}$  terms will remain constant for these processes. Indeed, with the exception of reverse electron transfer for the zinc rotaxane **2**, there is a global correlation between the rate constant for electron transfer and the inverse of the smallest energy gap ( $B_-$  or  $B_+$ ) as shown in Figure 5b. This might be construed to indicate that, with the one exception, the  $\beta_{AB}\beta_{BC}$  terms are similar for all the reactions.

It is interesting to consider the possibility that electron transfer via the singlet excited state of the zinc porphyrin in the zinc rotaxane **2** occurs by way of a two-step mechanism in which the reduced central zinc(II) complex appears as a real intermediate (reaction 7). There is no spectroscopic evidence to suggest involvement of such an intermediate, and the rate of appearance of the charge-transfer state exactly matches that of deactivation

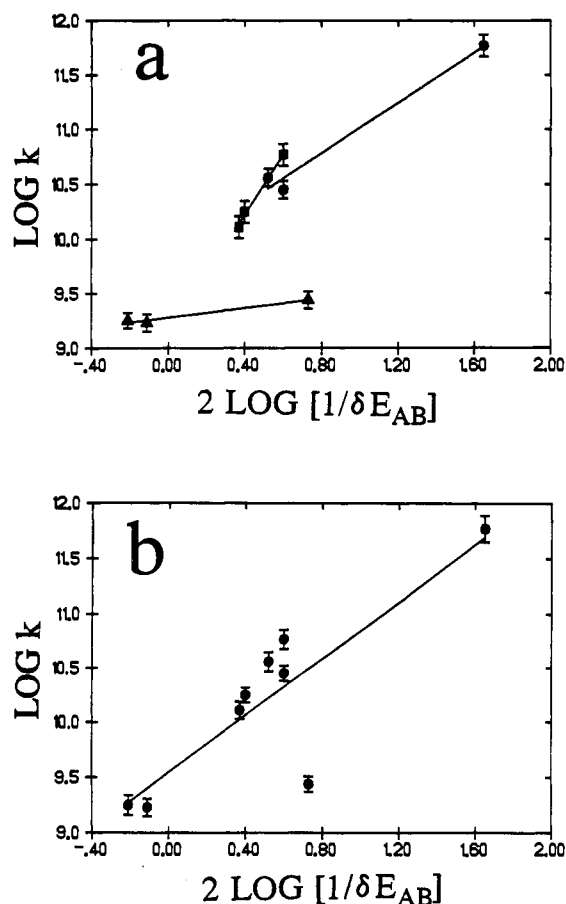


**Figure 5.** (a) Correlation between the rate constants for photoinduced electron transfer via the excited singlet state of the zinc porphyrin (●) and the excited triplet state of the gold porphyrin (■) and for reverse electron transfer (▲) and the inverse of the smallest energy gap for the rotaxanes in butyronitrile. (b) Global plot for all the electron-transfer rate constants versus the inverse of the smallest energy gap for the rotaxanes in butyronitrile.

of the zinc porphyrin excited singlet state. Even so, a two-step mechanism is possible if the lifetime of the intermediate is less than about 20 ps. It is anticipated that this possibility will be explored further and that low-temperature studies will be made to determine if the two reactions can be resolved by way of their possessing distinct activation energies.

Both the rates of electron transfer at zero activation free energy change ( $k_0$ ) and the magnitudes of the electronic coupling matrix element ( $V$ ) for the photoinduced reactions are substantially smaller in the cation-free rotaxane **3** than in the corresponding bis-porphyrin **4**. Since the respective energy gaps ( $B_-$  or  $B_+$ ) are assumed to be identical, the  $\beta_{AB}\beta_{BC}$  terms are expected to be smaller in the rotaxane. Indeed, calculation of the  $\beta_{AB}\beta_{BC}$  terms from eq 15 using the values of  $V$  derived from the temperature-dependence studies indicates that these terms are 5–8 times smaller than those found for the bis-porphyrin (Table IV).

This difference might arise from stereochemical changes imposed by the presence of the accessory 1,10-phenanthroline residue in the rotaxane; it is known that  $V$  depends on the stereochemistry of the spacer moiety<sup>38</sup> and (possibly) on the mutual orientation of the reactants.<sup>39</sup> Steric crowding by the accessory 1,10-phenanthroline residue may cause sufficient structural distortion to alter the geometry of the bis-porphyrin. Thus, changes in mutual orientation of the porphyrin rings with

(38) (a) Beratan, D. N.; Hopfield, J. J. *J. Am. Chem. Soc.* **1984**, *106*, 1584.

(b) Closs, G. L.; Miller, J. R. *Science* **1988**, *240*, 440.

(39) (a) Brocklehurst, B. *J. Phys. Chem.* **1979**, *83*, 536. (b) Siders, P.; Cave, R. J.; Marcus, R. A. *J. Phys. Chem.* **1986**, *90*, 1436. (c) Helms, A.; Heller, D.; McLendon, G. *J. Am. Chem. Soc.* **1991**, *113*, 4325.

respect to the spacer moiety may affect the  $\beta_{AB}\beta_{BC}$  terms and thereby modulate the rates of electron transfer. Alternately, the accessory 1,10-phenanthroline residue may affect the mutual orientation of the bridging phenyl rings and thereby change the level of electronic coupling between the porphyrin and spacer functions. It has been suggested that, for phenyl-bridged aromatic donor-acceptor systems,  $V$  depends on the angle between the  $\pi$ -systems.<sup>40,41</sup> Space-filling molecular models indicate that the pyrrolic substituents on the zinc porphyrin subunit in the rotaxanes force the phenyl ring to the more orthogonal than in the tetraarylporphyrin systems. It is likely, therefore, that the weaker electronic coupling in the rotaxanes relative to the bis-porphyrin arises from subtle changes in stereochemistry between the two systems. At room temperature, there is no indication that photoinduced electron transfer in the rotaxane **3** proceeds by way of the interspersed accessory 1,10-phenanthroline residue and, instead, reaction appears to involve a through-bond mechanism.

The derived  $V$  values are comparable for reverse electron-transfer reactions in the cation-free rotaxane **3** and the bis-porphyrin **4**, although the rate constant at zero activation free energy change is higher by a factor of 2 for the rotaxane. We have previously proposed<sup>14</sup> that this reaction in the bis-porphyrin may occur predominantly by a through-space mechanism. In this case, the presence of the accessory 1,10-phenanthroline residue in the rotaxane becomes especially important since it occupies much of the space between the reacting porphyrin subunits. This is probably the reason why the solvent reorganization energy for the rotaxane is only about half that found for the bis-porphyrin.

(40) Onuchic, J. N.; Beratan, D. N. *J. Am. Chem. Soc.* **1987**, *109*, 6771.

(41) Helms, A.; Heiler, D.; McLendon, G. *J. Am. Chem. Soc.* **1992**, *114*, 6227.

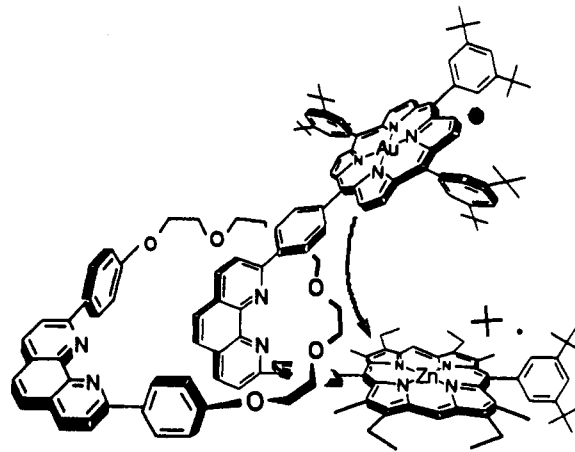


**Figure 6.** Schematic representation of the pathway for reverse electron transfer within the cation-free rotaxane **3**.

Charge recombination may involve orbitals resident on the accessory 1,10-phenanthroline residue, as depicted in Figure 6. This possibility will be studied further using rotaxanes which allow the overlap between the accessory residue and the porphyrin subunits to be varied in a more systematic fashion.

**Acknowledgment.** Support for this work was provided by the C.N.R.S., the National Science Foundation (CHE 9102657), and NATO (920916). The CFKR is supported jointly by the Division of Research Resources of the N.I.H. (RR00886) and by The University of Texas at Austin. We thank the U.S. Department of Energy for the award of a grant enabling construction of the sub-picosecond laser flash spectrometer.